First-Principles-Derived Dynamics of a Surface Reaction: Fluorine Etching of Si(100)

Paul C. Weakliem, Christine J. Wu, and Emily A. Carter
Department of Chemistry and Biochemistry, University of California, Los Angeles, California 90024-1569
(Received 14 February 1992)

We present a realistic simulation of the reaction of fluorine with Si(100). Isothermal molecular dynamics simulations, using an analytic many-body potential fit to first-principles quantum mechanical adsorbate-surface and experimental gas phase data, show the initial buildup of the fluorosilyl layer necessary for etching. Several aspects of the microscopic mechanism are revealed. These simulations represent the first time that first-principles-derived surface reaction dynamics have been carried out; we show that this approach is critical to obtaining physically correct results.

PACS numbers: 81.60.Cp, 82.20.Hf, 82.20.Kh, 85.40.Jq

Etching of silicon wafers often utilizes plasmas of fluorine-containing molecules [1], where the primary reactive species is thought to be F atoms [2]. Upon initial fluorine exposure, rapid adsorption of ~ 1.5 ML (monolayer) of F occurs [3]. Continued exposure then leads to a buildup of a fluorosilyl layer consisting of SiF, SiF_2, and SiF_3 [4-6]. This process ultimately culminates in steady-state etching at room temperature with production of mostly SiF_4, although some Si_2F_6 and Si_3F_8 also desorb from the surface [7-11].

Previous molecular dynamics (MD) simulations predicted that etching only occurs under extreme conditions: by melting the surface [12] or exposing it to high energy ($E_k > 3$ eV) F atoms [13]. We present a study of the initial stages of etching from MD simulations that utilizes a many-body potential energy function fit to high level first-principles quantum mechanical data. Our results differ starkly from previous studies, as described in the remainder of this Letter.

Previous MD simulations used the only available Si-F potential, which was developed by Stillinger and Weber (SW) [14], that consists of two- and three-body terms for every type of heteroatomic and homoatomic interaction. The terms have the general form of a polynomial modulated by an exponential that goes smoothly to zero at a cutoff. The SW potential for pure Si works well for both the bulk [15] and the (100) surface [16-18] and the Si-F potential is in reasonable agreement with experimental bond energies and geometries for the gas phase SiF_x ($x=1,2,3,4$) series. However, the Si-F heteroatomic terms were fitted only by SiF_x and Si_2F_6 properties (understandably, as those were the only data available for Si-F interactions), so it is not surprising that the potential fails to describe the interaction of F with Si surfaces correctly. With this in mind, two of us carried out first-principles quantum mechanical calculations of the interaction of multiple F atoms with embedded Si clusters constructed to represent pieces of the (100) surface, which is described in detail elsewhere [19,20]. We then compared the empirical SW potential to our highly correlated quantum mechanical data. The comparison for one approach of an F atom to the Si surface is illustrated in Fig. 1, where we see that although the functional form appears to be satisfactory [i.e., the shape of the dashed curve is similar to that of the quantum mechanical data (circles)], the depth of the SW well (0.25 eV) is in error by an order of magnitude compared to the quantum mechanical prediction of 3.0 eV. In general, every adsorption pathway and lateral interaction was predicted by the SW potential to be too repulsive (or not attractive enough) compared to the first-principles results, by up to 4 eV [21]. This explains why the SW potential only predicts etching under extreme circumstances: With the potential too repulsive, not enough F atoms can adsorb to

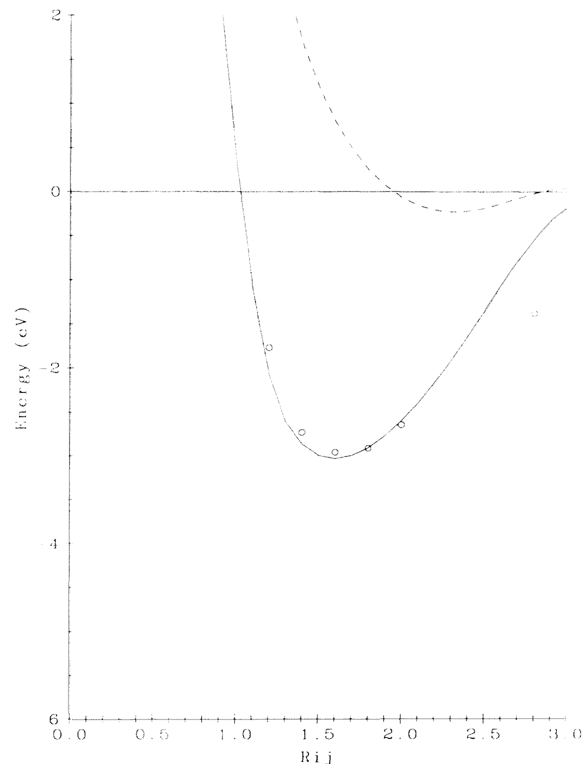

FIG. 1. Potential energy as a function of distance for the perpendicular approach of an F atom towards the center of a Si dimer bond. The dashed line is the SW potential [14], the circles are the first-principles quantum mechanical data [19,20], and the solid line is our new potential.

 © 1992 The American Physical Society

form the fluorosilyl layer necessary for etching.

Since the general shape of the potential appeared to be in reasonable agreement with the first-principles data, we decided to retain the functional form of the SW potential, and to refit it to 42 first-principles adsorbate-surface data points as well as to the experimental gas phase data for SiF_x ($x=1$-4) [22]. Since the homoatomic interactions seem to be adequate based on other studies [14,15,18], we modified the parameters, as well as a small change in the functional form, of the heteroatomic (cross) terms only. The two-body Si-F cross term is of the following form:

$$v_{SiF}=A_{SiF}(B_{SiF}r^{-3}-r^{-2})\exp[\gamma_{SiF}(r-a)^{-1}] \quad (0<r<a) \tag{1}$$

which vanishes beyond the cutoff a. The three-body cross terms consist of a sum of three terms depending on the angle at each of the three vertices and the adjacent sides of the triangle formed by a triplet of atoms. The three individual functions h, where θ is the angle and r and s are the lengths of the adjacent sides, have the form

$$h_{SiSiF}=A_{SiSiF}[(\cos\theta+\tfrac{1}{3})^2-c_{SiSiF}] \times\exp\{\gamma_{SiSiF}[(r-a)^{-1}+(s-a)^{-1}]\}, \tag{2}$$

$$h_{SiFSi}=A_{SiFSi}\exp\{\gamma_{SiFSi}[(r-a)^{-1}+(s-a)^{-1}]\}, \tag{3}$$

$$h_{SiFF}=A_{SiFF}\exp\{\gamma_{SiFF}[(r-a)^{-1}+(s-a)^{-1}]\}, \tag{4}$$

$$h_{FSiF}=A_{FSiF}[(\cos\theta-\cos 103°)^2-c_{FSiF}] \times\exp\{\gamma_{FSiF}[(r-a)^{-1}+(s-a)^{-1}]\}, \tag{5}$$

where each term again vanishes if either r or $s\geq a$. Note that the factor c_{SiSiF} in the h_{SiSiF} term is not present in the SW form of the potential.

Using the method of simulated annealing (SA) [23], we obtained approximately fifty candidate parameter sets. The predicted energetics and structures from these sets were then compared to both the first-principles quantum mechanical data and the available gas phase experimental data for the SiF_x molecules. Various Si_x-F_y potential curves were also examined to look for unphysical behavior for each set. The optimal set of parameters is given in Table I. As can be seen in Fig. 1 (solid line), this new parameter set fits these representative first-principles data (circles) quite well.

Using the modified SW potential with this new parameter set, we performed etching simulations in the same flavor as that of previous studies [12,24]. The Si(100) crystal was modeled by a periodically replicated (in the surface plane) five-layer slab with 32 atoms per layer in an adsorption probability study and 72 atoms per layer in a long time etching simulation. The top two layers evolved using a Verlet integration of the microcanonical (constant *NVE*) equations of motion, while the third and fourth layers were propagated with the Nosé canonical ensemble (constant *NVT*) algorithm to maintain a relatively constant temperature during this extremely exothermic reaction [18]. Both integrators used a time step of 0.25 fs. The bottom layer was held fixed to represent the infinite bulk lattice. The surface atoms were initially displaced to form the familiar $p(2\times1)$ rows of Si dimers [18], followed by thermal equilibration at 300 K. F atoms were introduced randomly at 6–8 Å above the surface for the adsorption probability studies and between 2 and 8 Å for the long time simulation, with random velocities corresponding to a temperature of $\sim$300 K. A reflective barrier was provided 14 Å above the surface to keep F atoms from escaping.

TABLE I. Parameters for heteroatomic terms.

Parameter	SW value	Our value
A_{SiF}	21.234 141 38	21.199 221
B_{SiF}	0.569 547 6433	0.546 418
γ_{SiF}	1.3	1.339 450
A_{SiSiF}	15.0	3.624 533
c_{SiSiF}	0.0	0.218 615
γ_{SiSiF}	1.0	0.463 088
A_{SiFSi}	50.0	50.874 092
γ_{SiFSi}	1.3	1.371 580
A_{SiFF}	2.5	2.792 073
γ_{SiFF} [a]	1.0	1.0
A_{FSiF}	24.0	22.406 434
c_{FSiF}	3.2	2.068 601
γ_{FSiF}	1.0	0.890 132

[a]This parameter was not permitted to change during the fitting process.

Adsorption probabilities at $\Theta_F=0$ and 1 ML were calculated from 100 5-ps trajectories at each coverage. For $\Theta_F=0$ ML, the new potential yields the same general results as the original SW potential [24], with an adsorption probability of $S_0=1.0$. These results are insensitive to which potential is used because the F atom is simply adding to the dangling bonds on the bare surface, a process that the original SW potential predicted as extremely favorable (SW predicts this to be 5.4 eV exothermic, while the first-principles value is 6.4 eV) [19,20]. The adsorption probability for $\Theta_F=1.0$ ML surface, where all Si dangling bonds were saturated with F atoms, was identically zero. As we discuss below, this negative result is key to understanding the etching mechanism.

The long time, room-temperature simulation is a more revealing test of our new potential because this simulation with the SW potential failed to predict any reactivity beyond saturation of the dangling bonds [12]. Thus, we performed two sets of *NVE*-*NVT* trajectories with identical initial conditions, one using the SW potential and one using our new potential. We exposed an equilibrated Si(100)-2×1 surface at 300 K initially to 10 gaseous F atoms and then added a single F atom every 62.5 fs, as described above. This was continued until there were 160 F atoms in the simulation cell. The temperature remained well below the melting point of Si throughout the

simulation.

In agreement with previous isothermal MD simulations [12], we find that simulations using the SW potential do not etch Si spontaneously, contrary to experiment. In particular, after 70 ps, the SW potential simulation resulted only in the formation of SiF species corresponding to 100% saturation of the Si surface dimer dangling bonds. No Si-Si bonds were broken, which is certainly a prerequisite for etching. In contrast, the simulations with our new potential predict rapid adsorption of ~ 1 ML of F within 10 ps, at which time a variety of SiF_x species have formed: 1 SiF_3, 3 SiF_2, and 65 SiF groups. Of this distribution, 3 SiF species are derived from second-layer Si atoms, while all other species formed from first-layer Si atoms. The makeup of this layer is consistent with x-ray photoemission (XPS) studies that suggest SiF_3 exists primarily near the surface while SiF dominates the SiF_x/Si interface region [25]. After the initial rapid adsorption, subsequent reaction of F with the Si surface occurs slowly. By 40 ps, several more surface SiF groups form; however, no further reaction occurs up to 95 ps.

The mechanism of formation of the fluorosilyl layer proceeds as follows. Initially, the F atoms attack the dangling bonds of the Si dimers on the surface, as seen in Fig. 2(a). However, even at a surface coverage of $\Theta_F = 0.5$ ML, Si-Si bonds are broken to form $SiF_{2(ad)}$ [Fig. 2(a), upper right] and F atoms begin reacting with second-layer atoms. F_2 is also observed to attack surface Si atoms. The release of ~ 10 eV of energy upon formation of SiF_2 causes nearby Si-Si bonds to break. In this trajectory, the resulting SiF_2 actually diffuses to a neighboring dangling bond on another Si atom. This exposed SiF_2 then rapidly forms SiF_3 [Fig. 2(b), bottom center], a precursor to SiF_4 or Si_2F_6 formation.

It is clear that disorder of the fluorinated surface is necessary for the buildup of the experimentally observed fluorosilyl layer, since chemisorption on a fully ordered 1-ML fluorinated surface does not readily occur. The long time etching simulation exhibits such disorder, even at low coverages, and indeed proceeds quickly to fluorine coverages above 1 ML. This disorder appears to be due to local heating of the surface caused by the F-Si reaction exothermicity. Si-Si bonds become vibrationally excited [Fig. 2(a), center right] and therefore are weakened and more susceptible to attack by incoming F atoms. Recent measurements of ~ 100 ps vibrational relaxation times for Si-H bonds on H-terminated Si(111) support the idea that energy transfer is slow through silicon [26] and thus local heating can be important on the time scale of surface reactions. This local heating also produces disorder in the surface and near surface Si layers [Fig. 2(b), lower left and right], a structural phenomenon recently observed via XPS by Yarmoff [27].

In conclusion, we have shown that by combining state-of-the-art first-principles quantum mechanical data with experimental data, a good potential for surface reaction dynamics can be obtained. Previous failures of the SW potential to model etching were due to a fit to an inadequate (gas phase only) database; the current refit of the potential to appropriate surface information yields a much better description for F-atom-Si surface interactions. Using molecular dynamics, we find an initial ad-

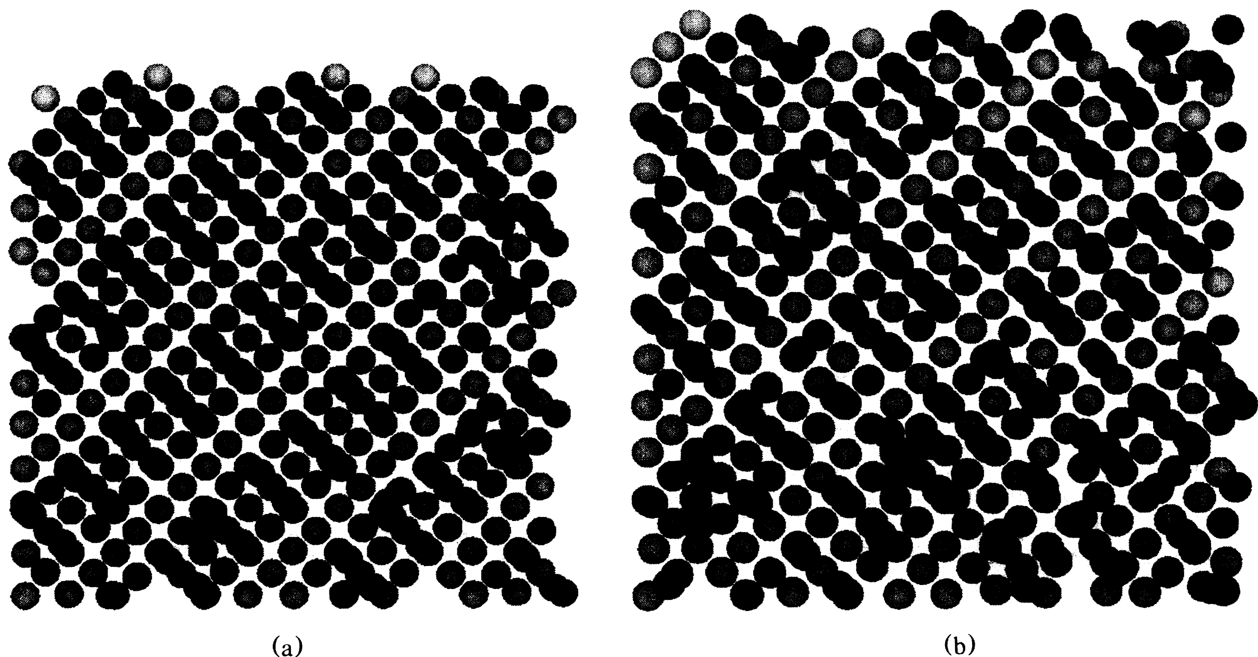

FIG. 2. Instantaneous configurations for the long time simulation. Red spheres are F atoms, blue spheres are Si atoms in the surface layer, green spheres are second-layer Si atoms, and yellow spheres are subsurface Si atoms: (a) $\Theta = 0.5$ ML and (b) $\Theta = 1.1$ ML.

sorption probability of unity, while $S=0$ for an ordered F monolayer. In long time simulations, we see the beginnings of the buildup of the fluorosilyl layer, with Si-Si dimer bond breaking occurring simultaneously with Si dangling bond saturation. Local heating clearly enhances formation of a disordered fluorosilyl network, which may be the key to steady-state etching, by continued replenishment of dangling bonds for fluorine to attack.

This work was funded by the Air Force Office of Scientific Research, the National Science Foundation, the Camille and Henry Dreyfus Foundation, and IBM.

[1] See H. F. Winters and J. W. Coburn, Surf. Sci. Rep. (to be published), for an excellent review of etching.
[2] J. W. Coburn and M. Chen, J. Appl. Phys. **51**, 3134 (1980).
[3] N. D. Shinn, J. F. Morar, and F. R. McFeely, J. Vac. Sci. Technol. A **2**, 1593 (1984).
[4] C. D. Stinespring and A. Freedman, Appl. Phys. Lett. **48**, 718 (1986).
[5] F. R. McFeely, J. F. Morar, and F. J. Himpsel, Surf. Sci. **165**, 277 (1986).
[6] H. F. Winters, J. W. Coburn, and T. J. Chuang, J. Vac. Sci. Technol. B **1**, 469 (1983).
[7] H. F. Winters and J. W. Coburn, Appl. Phys. Lett. **34**, 70 (1979).
[8] M. J. Vasile and F. A. Stevie, J. Appl. Phys. **53**, 3799 (1982).
[9] H. F. Winters and F. A. Houle, J. Appl. Phys. **54**, 1218 (1983).
[10] F. A. Houle, J. Appl. Phys. **60**, 3018 (1988).
[11] H. F. Winters and I. C. Plumb, J. Vac. Sci. Technol. B **9**, 197 (1991).
[12] F. H. Stillinger and T. A. Weber, Phys. Rev. Lett. **62**, 2144 (1989).
[13] T. A. Schoolcraft and B. J. Garrison, J. Am. Chem. Soc. **113**, 8221 (1991).
[14] T. A. Weber and F. H. Stillinger, J. Chem. Phys. **92**, 6239 (1990).
[15] F. H. Stillinger and T. A. Weber, Phys. Rev. B **31**, 5262 (1985).
[16] F. F. Abraham and I. P. Batra, Surf. Sci. **163**, L752 (1985).
[17] K. Khor and S. Das Sarma, Phys. Rev. B **36**, 7733 (1987).
[18] P. C. Weakliem and E. A. Carter, J. Chem. Phys. **96**, 3240 (1992).
[19] C. J. Wu and E. A. Carter, J. Am. Chem. Soc. **113**, 9061 (1991).
[20] C. J. Wu and E. A. Carter, Phys. Rev. B **45**, 9065 (1992).
[21] P. C. Weakliem and E. A. Carter, J. Chem. Phys. (to be published).
[22] R. Walsh, Acc. Chem. Res. **14**, 246 (1981).
[23] S. Kirkpatrick, J. C. D. Gelatt, and M. Vecchi, Science **220**, 671 (1983)
[24] T. A. Schoolcraft and B. J. Garrison, J. Vac. Sci. Technol. A **8**, 3496 (1990).
[25] C. W. Lo, D. K. Shuh, and J. A. Yarmoff (unpublished).
[26] M. Morin, P. Jokob, N. J. Levinos, Y. J. Chabal, and A. L. Harris, J. Chem. Phys. (to be published).
[27] J. A. Yarmoff (private communication).

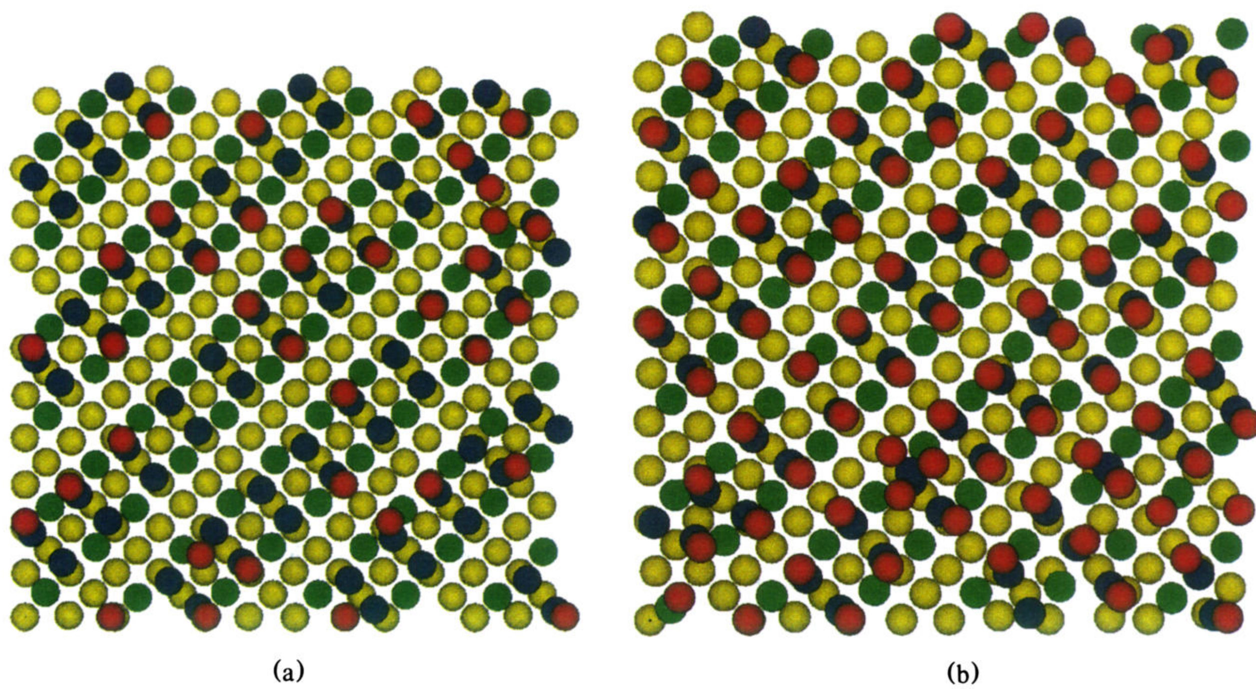

(a) (b)

FIG. 2. Instantaneous configurations for the long time simulation. Red spheres are F atoms, blue spheres are Si atoms in the surface layer, green spheres are second-layer Si atoms, and yellow spheres are subsurface Si atoms: (a) $\Theta = 0.5$ ML and (b) $\Theta = 1.1$ ML.